BIOLOGY OF REPRODUCTION **65,** 601–612 (2001)

Expression, Activity, and Subcellular Localization of Testicular Hormone-Sensitive Lipase During Postnatal Development in the Guinea Pig[1]

Ouafae Kabbaj,[3] Cecilia Holm,[4] María L. Vitale,[3] and R.-Marc Pelletier[2,3]

Département de Pathologie et Biologie Cellulaire,[3] Faculté de Médecine, Université de Montréal, Montréal, Québec, Canada H3T 1J4
Department of Cell and Molecular Biology,[4] Lund University, Lund S-223 62, Sweden

ABSTRACT

The present work reports on testicular hormone-sensitive lipase (HSL), the biological significance of which has been documented in male fertility. The HSL protein levels and enzymatic activity were measured, respectively, by densitometry of immunoreactive bands in Western blots, performed with antibodies against recombinant rat HSL, and by spectrophotometry in seminiferous tubules (STf) and interstitial tissue (ITf) enriched fractions generated from neonatal, pubertal, and adult guinea pig testes. In addition, HSL was studied in subcellular fractions obtained from STf isolated from adult testes and in epididymal spermatozoa (Spz). A 104-kDa HSL protein was detected in STf and ITf, the expression and activity of which increased with testicular development. Three immunoreactive bands of 104, 110, and 120 kDa were detected in the lysosomal subfraction, and two bands of 104 and 120 kDa were detected in Spz. The HSL activity was positively correlated with free (FC) and esterified (EC) cholesterol ratios in STf and ITf, but not with triglyceride (TG) levels, during testicular development. Immunolabeling localized HSL to elongated spermatids and Sertoli cells, where its distribution was stage-dependent, and within the cells lining the excurrent ducts of the testis. The findings of the 104- and 120-kDa HSL immunoreactive bands and of HSL activity in Spz as well, as the detection of the 104-, 110-, and 120-kDa immunoreactive bands in lysosomes, suggest that part of HSL may originate from germ cells and be imported in Sertoli cells. The HSL protein levels and enzymatic activity in ITf and STf were positively correlated with serum testosterone levels during development. To the best of our knowledge, this study is the first to contribute insights regarding the impact of HSL on FC:EC cholesterol ratios and TG levels in the interstitial tissue and tubules in relation to serum testosterone levels during postnatal development, and regarding the immunolocalization of the enzyme in regions of the male gamete consistent with spermatozoa-oocyte interaction.

male reproductive tract, Sertoli cells, spermatogenesis, testis

INTRODUCTION

Three main enzymes are implicated in the regulation of intracellular cholesterol metabolism. First, hormone-sensitive lipase (HSL) hydrolyzes esterified cholesterol (EC) and provides free cholesterol (FC) [1]. Second, acyl-coenzyme A:cholesterol acyl transferase is implicated in the esterification of cholesterol when the latter is present at concentrations exceeding metabolic demands [2]. Third, 3-hydroxy-3 methylglutaryl-coenzyme A reductase is the rate-limiting enzyme of the biosynthetic pathway of cholesterol [3].

The present study is focused on testicular HSL because of the manifest importance of the enzyme in male fertility. The HSL knockout mice (HSL−/−) have been generated to elucidate the role initially attributed to HSL in the development of obesity. However, these studies showed that HSL knockout male mice were sterile rather than obese, suggesting a key role of the enzyme in the testis [4]. A significant rise in cholesterol ester levels concomitantly with the absence of cholesterol esterase activity was reported in HSL−/− mouse testis [4]. These studies attest to the utmost biological significance of the enzyme in the maintenance of adequate cholesterol content in testicular cells.

The HSL is an intracellular enzyme, with a optimum pH of 7, that hydrolyzes cholesterol esters and triacylglycerol depending on its tissue location [5]. Several studies have shown that cholesterol ester hydrolase and HSL are identical proteins [1, 5–10]. Inhibition of cholesterol ester hydrolase causes an increase in the EC concentration of whole-mouse testis extracts and a decrease in the testosterone concentration of peripheral plasma [11]. The activity of HSL is regulated by reversible protein phosphorylation mediated by hormonal activation of the cAMP-dependent protein kinase [1]. The phosphorylated HSL is the active form [1].

Contribution of exogenous cholesterol to the seminiferous tubules requires the participation of factors, either enzymatic or of another nature, to regulate the concentration of the compound to levels that are consistent with the production of viable and fertile male gametes in the tubules. Little information is available regarding the origin, hydrolysis, esterification, synthesis, storage, mobilization, and transport of cholesterol within the tubules, despite the report that important amounts of cholesterol reside within the tubules themselves [12]. To correct this shortage of information, the present study emphasized the physiological significance of HSL-induced hydrolysis of cholesterol inside the tubules. Because previous studies of testicular HSL [10, 13–16] have generally been carried out using whole-testis extracts, those studies provided little information regarding the respective participation of each of the two cellular compartments of the testis. We hypothesize that HSL regulates FC:EC ratios distinctly in the interstitial space and in the neighboring tubules. If the hypothesis is correct, this should allow us to correlate HSL-induced changes in FC:EC ratios with a physiological event typical either of the interstitial tissue or of the tubules and with a particular phase of post-

[1]Supported in part by NSERC grant OGP0041653 to R.M.P. and by NSERC grant OGP0194652 to M.L.V.; M.L.V. is also funded by a scholarship from Fonds de la Recherche en Santé du Québec.
[2]Correspondence: R.-Marc Pelletier, Département de Pathologie et Biologie Cellulaire, Faculté de Médecine, Université de Montréal, 2900 Édouard-Montpetit, Montréal, QC, Canada H3T 1J4. FAX: 514 485 7932; e-mail: marc.pelletier@umontreal.ca

Received: 14 December 2000.
First decision: 31 January 2001.
Accepted: 5 April 2001.

ISSN: 0006-3363. http://www.biolreprod.org

natal development, namely, a peak in serum testosterone levels in the adult and meiosis during puberty. Here, for the first time, HSL expression and activity were measured in interstitial tissue enriched fractions (ITf) and seminiferous tubule enriched fractions (STf) generated from extracts of whole testes harvested during the neonatal period, puberty, and adulthood. The sublocalization of the enzyme was achieved for the first time using subcellular fractions generated from STf obtained from adult testes. To the best of our knowledge, the present study is the first to contribute insights regarding the impact of HSL on FC:EC ratios and triglyceride (TG) levels in the interstitial tissue and tubules in relation with serum testosterone levels during postnatal development, and regarding immunolocalization of the enzyme in regions of the male gamete consistent with spermatozoa-oocyte interaction.

MATERIALS AND METHODS

Animals

We used testes obtained from 6-day-old neonatal, 11- and 21-day-old pubertal, and adult guinea pigs aged more than 54 days. All guinea pigs were from the Hartley strain and were purchased from Charles River (St-Constant, PQ, Canada). Five animals were used per age group. Animals were anesthetized by i.p. injection of 0.9 ml/kg body weight of sodium phenobarbital (Somnotol; MCI Pharmaceutical, Mississauga, ON, Canada). The protocol was approved by the Université de Montréal Animal Care Committee.

Source of Chemicals

Acetonitrile, BSA, dithioerythritol, glucose-6-phosphate, metrizamide, imidazole, *p*-iodonitrotetrazolium violet (INT), *p*-nitrocatechol, nitrocatechol sulfate, *p*-nitrophenylbutyrate (PNPB), PMSF, sodium succinate, sucrose, soybean trypsin inhibitor, fluorescein isothiocyanate (FITC)-anti-rabbit IgG, 1,4-diazabicyclo-(2,2,2)-octane (DABCO), and the TG kit were purchased from Sigma (St. Louis, MO). Antipain, aprotinin, collagenase D, Western blot development kit Lumi-light^{plus}, leupeptin, and pepstatin were obtained from Boehringer Mannheim (Laval, QC, Canada). Minimum essential medium (MEM) was from Gibco BRL (Burlington, ON, Canada). The testosterone ELISA kit was purchased from American Laboratory Products Co., Ltd. (Windham, NH). Biotinylated anti-rabbit IgG and horse radish peroxidase (HRP)-conjugated streptavidin were purchased from Amersham Bio/Can Scientific (Mississauga, ON, Canada).

Source of HSL Antibodies

Antibodies against homogenous recombinant rat HSL were generated in rabbits [17]. Rabbit antiserum was affinity-purified against the recombinant rat HSL coupled to a cyanogen bromide (CNBr)-activated Sepharose 4B column (Amersham Pharmacia Biotech, Solna, Sweden). The affinity-purified antibodies were specific for HSL and did not cross-react with other proteins on Western blot analyses of tissue extracts.

Controls

The specificity of HSL antibody was tested using guinea pig adipose tissue obtained from the anterior abdominal wall as a positive control. For negative controls, preimmune serum as well as the primary or secondary antibody alone were used. The HSL antibody was also preadsorbed with rat adipose tissue to ascertain that the HSL immunoreactivity detected in guinea pig tissues corresponded to HSL.

Isolation of STf and ITf

Freshly decapsulated testes were incubated with 0.25 mg/ml of collagenase D and 0.1 mg/ml of soybean trypsin inhibitor in MEM in a water-shaker bath set at 80 cycles/min and 37°C. The reaction was stopped by addition of an equal volume of MEM. The seminiferous tubules were allowed to settle by gravity, whereas interstitial cells occupied the supernatant. Further separation was achieved by centrifugation at 600 rpm in a GS-6R Beckman centrifuge equipped with a GH 3.8 rotor (Beckman, Mississauga, ON, Canada) for 20 min. The STf and ITf obtained were washed twice in PBS (137 mM NaCl, 3 mM KCl, 8 mM Na_2HPO_4, and 1.5 mM KH_2PO_4 [pH 7.4]) and homogenized on ice with a glass tissue grinder in PBS containing 2 mM PMSF, 1 mM EDTA, 2 μg/ml of leupeptin, and 2 μg/ml of aprotinin. The purity of the tubule and interstitial cell fractions was evaluated by light microscopy.

Subcellular Fractionation

The STf isolated from three adult guinea pig testes were pooled and submitted to a multistep centrifugation protocol as described initially by De Duve et al. [18] and Wattiaux et al. [19]. The STf were homogenized in three volumes of sucrose buffer (0.25 M sucrose, 4 mM imidazol [pH 7.4], and 1 mM PMSF) with a glass homogenizer. The homogenate was centrifuged at 700 × *g* for 10 min using a GS-6R Beckman centrifuge equipped with GH 3.8 rotor. The supernatant was saved, and the pellet was then resuspended and recentrifuged as described above. The process was repeated a third time, and the three supernatants were pooled. The resulting pellet contained the nuclear subfraction. The pooled supernatants were centrifuged at 3000 × *g* for 10 min, and the resulting pellet constituted the heavy mitochondrial subfraction. The supernatant was centrifuged at 82 000 × *g* for 7 min to pellet the light mitochondrial subfraction (lM). The supernatant of this last centrifugation was then centrifuged at 110 000 × *g* for 1 h to pellet the microsomal subfraction (Mc), and the supernatant constituted the cytosolic subfraction. The lM and Mc subfractions were obtained using a Beckman ultracentrifuge XL-70 (Beckman, Palo Alto, CA) equipped with a fixed rotor (type 50 Ti). The lM was resuspended in 30% metrizamide and placed in the bottom of a discontinuous gradient made of 26%, 24%, and 19% (w/v) metrizamide and then centrifuged at 95 000 × *g* for 2 h. Lysosomes were recovered in 19%–24% (w/v) interface [20] and resuspended in an equal volume of sucrose buffer. In addition, the Mc was used for separation of the Golgi apparatus, smooth endoplasmic reticulum (sER), and rough endoplasmic reticulum (rER) subfractions using the method described by Bergeron et al. [21] and Paiement et al. [22]. The Mc was suspended in sucrose to give a final concentration of 1.38 M sucrose; placed under a step-gradient of 1.0, 0.86, and 0.25 M sucrose; and centrifuged at 300 000 × *g* for 1 h. The Golgi subfraction was recovered from 0.25 to 0.86 and 0.86 to 1.0 M interfaces. The residual load-zone fraction contained the sER and the residual pellet the rER. The lysosomes, Golgi apparatus, sER, and rER were obtained using a Beckman ultracentrifuge XL-70 equipped with a SW60 rotor.

Biochemical Characterization of Subcellular Fractions

For biochemical characterization of enriched subfractions, the activities of the following specific enzymes were measured in each different subcellular fraction: arylsulfatase and acid phosphatase (lysosomes), succinate dehydrogenase (mitochondria), and glucose-6-phosphatase (microsomes). For arylsulfatase determination, samples of different subcellular fractions were solubilized in 1% Triton X-100 and incubated with 10 mM of the inorganic substrate *p*-nitrocatechol sulfate for 30 min at 37°C. Arylsulfatase activity was measured by determining the absorbance of the sample at 515 nm and comparison with a nitrocatechol standard curve [20, 23]. Acid phosphatase was assayed as described by Graham [24]. Samples of different subfractions were incubated with *p*-nitrophenyl phosphate as substrate. The reaction was stopped by addition of 0.25 M NaOH. Released phosphate was measured according to the method described by Ames and Dubin [25] using inorganic phosphate as standard. Succinate dehydrogenase was assayed as described by Davis and Bloom [26] and by Graham [24]. Samples of different subcellular fractions were incubated for 10 min at 37°C with sodium succinate as substrate and INT as an artificial electron acceptor. The reaction was stopped by adding ethyl acetate:ethanol:trichloracetic acid (TCA) (5:5:1, v:v:w). Glucose-6-phosphatase was measured as described by Graham [24]. Samples were incubated with 0.1 M glucose-6-phosphate as substrate for 30 min at 37°C, and the reaction was stopped by addition of ice-cold, 8% (w:v) TCA. Released phosphate was assayed as described above for measurement of acid phosphatase activity.

Epididymal Spermatozoa

Epididymal spermatozoa were flushed from the cauda or tail of epididymides from adult guinea pigs by perfusion of cold PBS. Spermatozoa were washed twice in PBS and recovered by centrifugation at 1000 rpm for 4 min (GS-6R Beckman centrifuge). Spermatozoa were resuspended in 10 mM Tris-HCL (pH 8) containing 1 mM EDTA for 5 min to lyse contaminating epithelial and blood cells [27]. For Western blot analyses, spermatozoa were diluted 1:1 v:v in cold PBS containing 2 mM PMSF, 1 mM EDTA, 2 μg/ml of leupeptin, and 2 μg/ml of aprotinin and then

sonicated while in ice using a sonic dismembrator (model 300; Fisher, Farmington, NY) at maximal setting during three consecutive intervals of 30 sec each. For immunofluorescence studies, spermatozoa were treated with diluted 1:5 v:v in PBS and processed as described below.

Protein Determination

Proteins in the samples were measured according to the method described by Bradford [28] using a Bio-Rad reagent (Bio-Rad, ON, Canada) and BSA as the standard.

Electrophoresis and Western Blots

Proteins in the homogenates were denatured in a buffer containing 8 mM urea, 3% SDS, 5% β-mercaptoethanol, 7 mM Tris-HCl (pH 7.6), and 0.005% bromophenol blue, followed by heating at 100°C for 2 min. Between 20 and 30 μg of total proteins were loaded on a 10% polyacrylamide minigel. Electrophoresis was conducted at 100 V for 2 h [29]. Proteins were then electrotransferred onto nitrocellulose membranes [30]. Samples obtained by subcellular fractionation were treated in the same manner. When adipose tissue was used as a positive control, only 5 μg of total proteins were utilized, because HSL is very abundant in this tissue. Membranes were blocked with 5% skim milk in Tris-buffered saline (TBS: 140 mM NaCl and 50 mM Tris-HCl [pH 7.4]) for 60 min at 37°C and then incubated with anti-HSL (1:150 dilution in 5% skim milk-TBS) for 2 h at 37°C. Membranes were thoroughly rinsed and incubated with an anti-rabbit IgG peroxidase conjugate (1:2000 dilution in 5% skim milk in TBS) as previously described [29]. The membranes were incubated with enhanced chemiluminescence detection reagents before exposure to x-ray films.

Preparation of Tissues for Immunolocalization of HSL

Testes were first fixed by perfusion of 15 ml of PBS (pH 7.4) through the testicular artery, followed by 60 ml of Bouin fixative [31]. Then, tissues were further immersed in the same fixative mixture for 36–48 h at room temperature (RT) [29, 32, 33]. Tissues were dehydrated in ethanol and in xylene before paraffinization. Tissue sections were mounted on glass slides coated with 3-aminopropyltriethoxysilane and exposed to 0.6% hydrogen peroxide (H_2O_2) in TBS containing 0.1% Tween 20 (TBST) to inhibit potential endogenous peroxidase activity.

Immunolabeling

To block nonspecific binding, sections were first incubated for 1 h at RT with 0.5% skim milk in TBST and next incubated overnight at RT with anti-HSL antibodies (1:35 dilution) and then for 1 h with biotinylated anti-rabbit IgG (1:1000 dilution) followed by HRP-conjugated streptavidin (1:200 dilution). The sections were washed in TBST after each incubation and exposed to TBS containing 0.01% H_2O_2 and 0.05% diaminobenzidine tetrachloride (pH 7.7) for 10 min at RT [29, 33]. The sections were washed in water, counterstained with a 0.05% aqueous methylene blue, and mounted in Permount (Fisher Scientific, Pittsburgh, PA). The recording of the stage-dependent distribution of HSL in adult guinea pigs were made using the identification method of the stages of the seminiferous epithelium cycle proposed by Clermont [34].

Immunofluorescence

The spermatozoa were seeded on poly-L-lysine-coated cover slips and air-dried. Spermatozoa were fixed with −20°C methanol for 10 min, dried, and washed twice in PBS before being incubated with 3% skim milk in PBS for 1 h at 37°C as described elsewhere [29] to prevent nonspecific binding. The cells were washed in PBS and incubated with a 1:6 dilution of anti-rat HSL prepared in 1% skim milk in PBS for 1 h at 37°C. The cover slips were washed with PBS, incubated with FITC-conjugated anti-rabbit IgG antibody (1:400 dilution in 1% BSA) in PBS at 37°C for 1 h and washed. Controls included incubation of cell preparations with preimmune serum or with the secondary antibody alone. The cover slips were mounted in PBS:glycerol (1:1) containing 5% DABCO before being viewed with a Carl Zeiss (Thornwood, NY) fluorescence Axiophot. Pictures were taken with TMAX 400 ASA Kodak films (Eastman Kodak Co., Rochester, NY).

HSL Activity

The HSL activity was assayed using PNPB as substrate [35]. The STf, ITf, and adipose tissue were homogenized on ice in 0.25 M sucrose, 1 mM EDTA (pH 7.0), 1 mM dithioerythreitol, 20 μg/ml of leupeptin, 2 μg/ml of antipain, and 1 μg/ml of pepstatin. Ten to twenty μg of total proteins of each sample were incubated with PNPB (diluted in acetonitrile) and buffer (0.1 M NaH_2PO_4, 0.9% NaCl, and 1 mM dithioerythreitol [pH 7.25]) for 10 min at 37°C. The addition of 3.25 ml of methanol:chloroform:heptane mixture (10:9:7) stopped the reaction. After centrifugation at 800 × *g* for 20 min, the absorbance of the supernatant was measured at 400 nm in a spectrophotometer (UV 160; Shimadzu Corporation, Kyoto, Japan). The enzymatic activity was expressed in units, with one unit being equivalent to the release of 1 μmol of *p*-nitrophenol per minute. All samples were analyzed in triplicate, and HSL activity was related to the total protein concentration of the sample.

Determination of FC and EC Concentrations in STf and ITf

Lipids in the samples were extracted in hexane:isopropanol (3:2, v:v) containing the internal standard stigmasterol and stigmasteryl oleate at RT. Lipids extracts were dried under N_2, resuspended in chloroform, and separated on silica G, 250-μm, thin-layer chromatographic (TLC) plates with hexane:diethyl ether:NH_4OH (c) (80:20:1) as solvent. The separated lipids were visualized by briefly placing the TLC plate in a chamber of iodine vapors. Areas corresponding to the separated cholesterol and cholesteryl esters were labeled, and the iodine was allowed to sublime. The areas containing cholesterol, which also contained the stigmasterol internal standard, were scraped into a glass tube containing chloroform:methanol (2:1). The mixture was then vortexed, centrifuged at low speed, and the supernatant removed and saved for future analyses. The cholesteryl ester bands, which also contained the stigmasteryl oleate internal standard, were scraped into a glass tube and hydrolyzed in KOH by heating at 80°C for 30 min. After cooling, 0.5 ml of H_2O and 1 ml of hexane were added, the mixture was vortexed, and the phases were separated by low-speed centrifugation. The upper hexane layer containing the cholesterol (and the internal standard stigmasterol) was removed and saved for future analyses [36].

The cholesterol samples were analyzed by gas-liquid chromatography (6890 series; Hewlett-Packard, Boise, ID) as described by Brown et al. [37] using a Supelco SPB 1701 column (Sigma-Aldrich, Oakville, ON, Canada). Average elution time for cholesterol and stigmasterol were 17 and 22.5 min, respectively. Quantification was performed by reference to the internal standard stigmasterol. The sensitivity of the method was 4 ng of cholesterol.

Determination of TG Concentrations in STf and ITf

Quantification of TG from the STf and ITf was carried out using a TG kit (Sigma-Aldrich) according to the protocol of the manufacturer. Briefly, TG were hydrolyzed to glycerol and free fatty acids by incubation with a lipase. The glycerol produced was measured by coupled enzyme reactions catalyzed by glycerol kinase, glycerol phosphate oxidase, and peroxidase. The sensitivity of the method was 0.01 g/L of glycerol.

Serum Testosterone Concentration

Serum levels of testosterone were measured by ELISA using commercially available kits according to the recommendation of the manufacturer (American Laboratory Products). The sensitivity of the method was 0.07 ng/ml.

Data Analysis and Statistical Analysis

The relative HSL protein content of scanned immunoreactive bands in Western blots was estimated by densitometry (Scion Image Software; Scion Corporation, Frederick, MD). The bands were scanned using a laser scanner (Astra 1200S; Umax Data System Inc., Hsinchu, Taiwan, ROC). Descriptive statistics are presented in the form of figures with mean ± SEM. Pearson correlation coefficients were calculated for subsets of variables that were observed in the same animals. Analysis of variance for repeated measures was carried out, with age as the between-subjects factors and variables of the same type and scale as the within-subject factors (FC and EC, or HSL activity in STf and ITf). For variables of different types (e.g., FC and TG, EC and TG, or HSL activity and testosterone), a multivariate one-way design was used, with age as the factor and the variables as the components of the response vector. Post-hoc comparisons (*t*-tests) between age groups were performed with the Bonferroni (Dunn) method. When necessary, logarithmic transformation were applied. The significance level of 0.05 was used. All analyses were carried out with the SAS software (SAS Institute, Cary, NC).

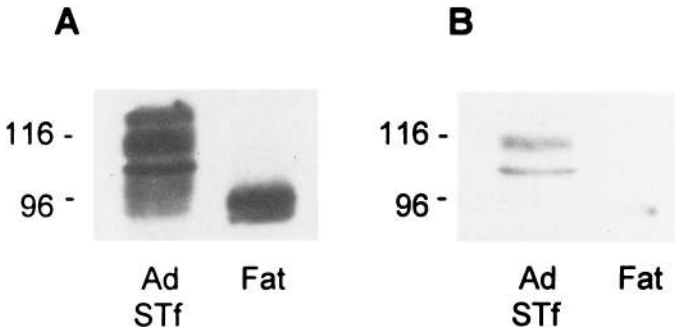

FIG. 1. Control for anti-rat HSL immunoreactivity in guinea pig tissues. Samples of adult (Ad) guinea pig STf and adipose tissue (Fat) were homogenized, and 20 μg of total STf proteins and 5 μg of total adipose tissue proteins were subjected to SDS-PAGE and Western blotting. The membrane was incubated with anti-rat HSL (**A**) or with anti-rat HSL antibody preadsorbed with rat adipose tissue (**B**). All immunoreactive bands detected in guinea pig tissues were less intense when the membrane was incubated with the preadsorbed HSL antibody than when incubated with the nontreated antibody.

RESULTS

Western Blot Analyses

Controls using anti-HSL preadsorbed with rat adipose tissue showed a considerable decrease of HSL immunoreactivity in guinea pig testis and adipose tissue extracts (Fig. 1), indicating that the HSL immunoreactivity detected in guinea pig tissues was due to presence of the enzyme.

The presence of HSL in the ITf and STf obtained from neonatal (6-day-old), pubertal (11- and 21-day-old), and adult (>55 days) guinea pig testes and in epididymal spermatozoa was studied by Western blot analyses. In this species, spermatogenesis has been reported to start approximately 7 days after birth and to be completed approximately 42–45 days after birth [38]. The blots showed a band at 104 kDa in the ITf and STf (Fig. 2A, arrowhead). The molecular mass of HSL detected in the ITf and STf was slightly greater than that in the adipose tissue (90 kDa)

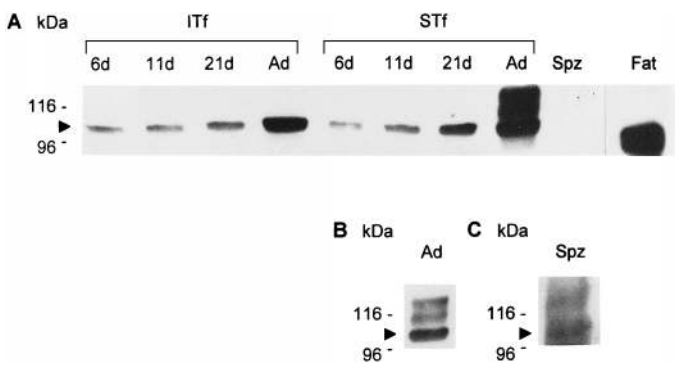

FIG. 2. Western blot analyses of HSL in ITf and STf enriched fractions during postnatal development. The ITf and STf were prepared from neonatal (6-day-old), pubertal (11- and 21-day-old), and adult (Ad) guinea pig testes. Adipose tissue (Fat) was used as a positive control. The figure shows a representative Western blot. **A**) An immunoreactive band with a molecular mass of 104 kDa (arrowhead) was detected in testicular samples, whereas in the adipose tissue, the immunoreactive band showed a molecular mass of 90 kDa. The intensity of the HSL band at 104 kDa increased with age in STf and ITf. Two additional immunoreactive bands of 110 and 120 kDa were detected in the STf obtained from the adult testes. **B**) The bands were apparent even in briefly exposed membranes. **C**) In epididymal spermatozoa (Spz), one HSL immunoreactive band of 104-kDa and another of 120-kDa molecular mass were detected in overexposed membranes. d, Days.

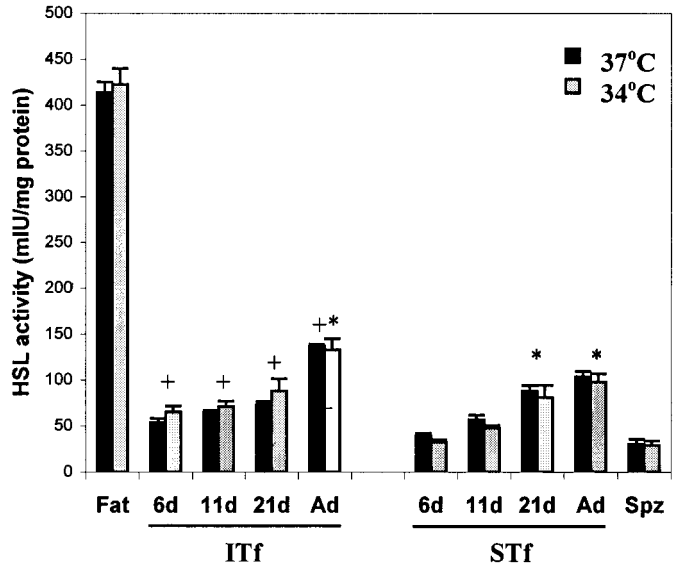

FIG. 3. The HSL activity during postnatal development in ITf and STf. The HSL activity was assayed at 34°C and at 37°C in ITf and STf obtained from neonatal (6-day-old), pubertal (11- and 21-day-old), and adult (Ad) guinea pig testes. Adipose tissue (Fat) was used as a positive control. The samples were assayed in triplicate, and the data shown are the mean ± SEM of three independent experiments. The HSL activity increased with age in both the ITf and STf. The HSL activity in these two enriched fractions was significantly higher in the samples from adult testes than in samples from 6-day-old testes (*$P < 0.05$). In addition, HSL activity was higher in the STf from the 21-day-old testis than in that from the 6-day-old testis. The HSL activity in the ITf of 6-, 11-, and 21-day-old as well as adult testes was higher than that measured in the STf of the same age groups (+$P < 0.05$). The HSL activity was detected in epididymal spermatozoa (Spz). No significant differences were detected between HSL activities assayed at 34°C and at 37°C in ITf, STf, and Spz.

(Fig. 2A). The intensity of the 104-kDa band was highest in the ITf and STf from adults (Fig. 2A). Two additional immunoreactive bands of 110 and 120 kDa were detected only in the STf obtained from adult testes (Fig. 2, A and B). These bands were not detected in STf from other age groups or in the ITf of the adult group, even when membranes were overexposed. Two HSL immunoreactive bands of 104 and 120 kDa were detected in spermatozoa when membranes were overexposed (Fig. 2C).

HSL Activity

Previous studies had reported that the activity of testicular cholesterol ester hydrolase was temperature sensitive [39–41]; therefore, we compared the HSL activity measured at the scrotal temperature (34°C) with the enzymatic activity measured at the body temperature (37°C). No significant differences were detected between the HSL activity assayed at 34°C and that assayed at 37°C in ITf and STf (Fig. 3). The HSL was active in the ITf and STf in all age groups studied (Fig. 3). The HSL activity was higher in adipose tissue than in the ITf and STf of all age groups. The HSL activity was significantly higher in the ITf of the adult testes and in the STf of the 21-day-old and adult testes than in the same fractions of the 6-day-old guinea pig testes ($P < 0.05$). The HSL activity in the ITf of the 6-, 11-, and 21-day-old and adult testes was higher than that in the STf of the same age groups ($P < 0.05$). The HSL was active in epididymal spermatozoa (Fig. 3).

The increase in HSL enzymatic activity paralleled the increase in HSL protein levels in all age groups studied,

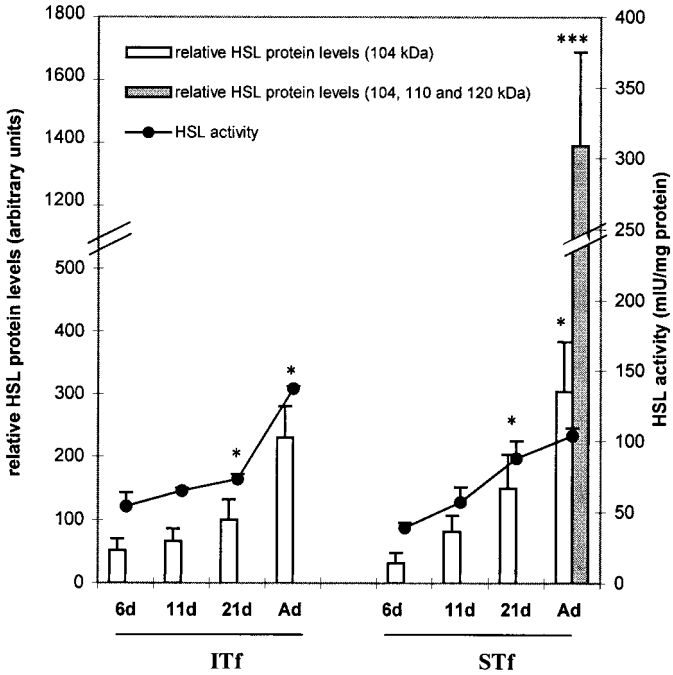

FIG. 4. The HSL activity and relative HSL protein levels during postnatal testicular development. The 104-kDa HSL immunoreactive bands in the ITf and STf of Western blots were scanned, and the intensity of the bands was quantified by densitometry using the Scion Image Software. The optical density of the bands (open rectangles) was expressed in arbitrary units and compared with the HSL activity (solid lines joined by closed circles). Both HSL activity and HSL concentration increased with age in the ITf and STf. The HSL activity and HSL concentration were significantly higher in the ITf and STf from the 21-day-old and adult testes than in those from the 6-day-old testes (*$P < 0.05$). When all three immunoreactive bands (104, 110, and 120 kDa) were considered in adult STf samples, the relative HSL concentration was even more significantly higher in the STf of the adult testes than in that of the 6-day-old testes (***$P <$ 0.001 vs. 6-day-old samples).

except in the STf of the adult testis, in which HSL protein levels increased more than the HSL enzymatic activity ($P < 0.05$) (Fig. 4). The relative enzyme concentration increased even more when the three bands were considered in the STf of the adult testes (Fig. 4), reaching 12.5-fold the value recorded in the STf of the 6-day-old testes ($P < 0.001$ vs. 6-day-old sample).

Subcellular Distribution of HSL in STf

To determine the subcellular localization of HSL, STf obtained from adult testes were homogenized and subjected to subcellular fractionation. The subfractions were characterized by their specific enzyme markers (Table 1). The enzymatic profile of the various subcellular fractions revealed an enrichment of arylsulfatase and acid phosphatase activities in the lysosomal subfraction, an enrichment of succinate dehydrogenase in the mitochondrial subfraction, and an enrichment of the glucose-6-phosphatase in the Mc (Golgi apparatus, sER, and rER). All subfractions contained low levels of the other enzymes, indicating low levels of contamination with the other subfractions.

The 104-kDa HSL was detected in the STf total homogenate as well as the cytosolic and lysosomal subfractions, and traces of the enzyme were found in the sER, but not in the other subcellular fractions studied (Fig. 5, arrowhead). The 110- and 120-kDa immunoreactive bands detected in the STf total homogenate were observed only in the lysosomal subfraction (Fig. 5, arrows).

TABLE 1. Distribution of marker enzyme activities in tubule subcellular fractions.[a]

Subfractions	Arylsulfatase	Acid phosphatase	Succinate dehydrogenase	Glucose-6-phosphatase
Nuclei	0.30	1.31	6.10	1.03
Mitochondria	0.91	1.19	5.16	0.47
rER	1.06	2.18	0.00	2.32
sER	0.00	1.50	0.00	7.65
Golgi	0.00	1.50	0.00	21.60
Lysosomes	6.00	7.12	1.19	1.35
Cytosol	0.01	0.01	0.00	0.98

[a] The activity of specific enzymes was measured in each different subcellular fraction for biochemical characterization of the enriched fractions: arylsulfatase and acid phosphatase for the lysosomal subfraction, succinate dehydrogenase for the mitochondrial subfraction, and glucose-6-phosphatase for the microsomal (rER, sER, and Golgi apparatus) subfraction. The data showed the enrichment of arylsulfatase and acid phosphatase activities in the lysosomal subfraction, the enrichment of succinate dehydrogenase in the mitochondrial subfraction, and the enrichment of the glucose-6-phosphatase in the microsomal subfraction. All subfractions contained low levels of other nonspecific enzymes, suggesting low contamination with the others subfractions. Enzymatic activities are expressed as % enzyme activity/% total proteins.

FC, EC, and TG Variations in STf and ITf

Lipids were first extracted and separated by TLC, and FC and EC were quantified by gas-liquid chromatography. The FC:EC ratios were roughly the same (near three) in ITf and STf in the adult; however, at the onset of development (6-day-old group), the ratios neared two in the STf and one in the ITf (Fig. 6). The FC and EC levels decreased in the ITf and STf with postnatal testicular development, but the decrease was significant only for EC in the ITf of the adult ($P < 0.05$ vs. the 6-day-old sample) (Fig. 6). The FC:EC ratios increased with testicular development and reached 152% and 326% in the STf and ITf, respectively, of the value recorded in the same fractions in the 6-day-old testes (Fig. 6). The FC:EC ratios paralleled the increase in the HSL activity assessed by hydrolysis of PNPB in the STf ($r = 0.80$, $P < 0.01$, n = 10) and ITf ($r = 0.71$, $P < 0.05$, n = 10) (Fig. 6).

The TG concentrations were measured in the STf and ITf in all age groups (Fig. 7). The TG levels did not vary significantly during development (Fig. 7), and no correlation was detected between the HSL activity and TG levels in the STf ($r = -0.27$ [not significant]) and ITf ($r = -0.34$ [not significant]).

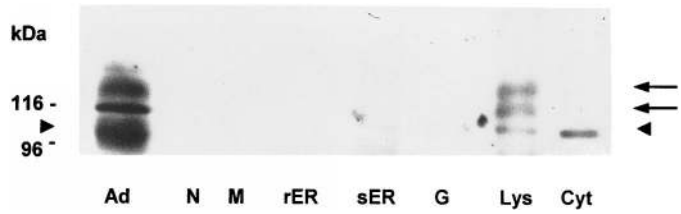

FIG. 5. Western blot analysis of HSL in subcellular fractions obtained from STf of adult testes. In the STf from adult testes (Ad), three HSL immunoreactive bands with molecular masses of 104 (arrowhead), 110, and 120 kDa (arrows) were present. In the subcellular fractions from the STf of adult testes, three bands with molecular masses of 104, 110, and 120 kDa were detected in the lysosomal subfraction (Lys). In the cytosolic subfraction (Cyt), only the 104-kDa immunoreactive band was detected. Traces of the 104-kDa band were detected in the sER. No HSL immunoreactivity was detected in the nuclear (N), mitochondria (M), rER, and Golgi apparatus (G) subfractions.

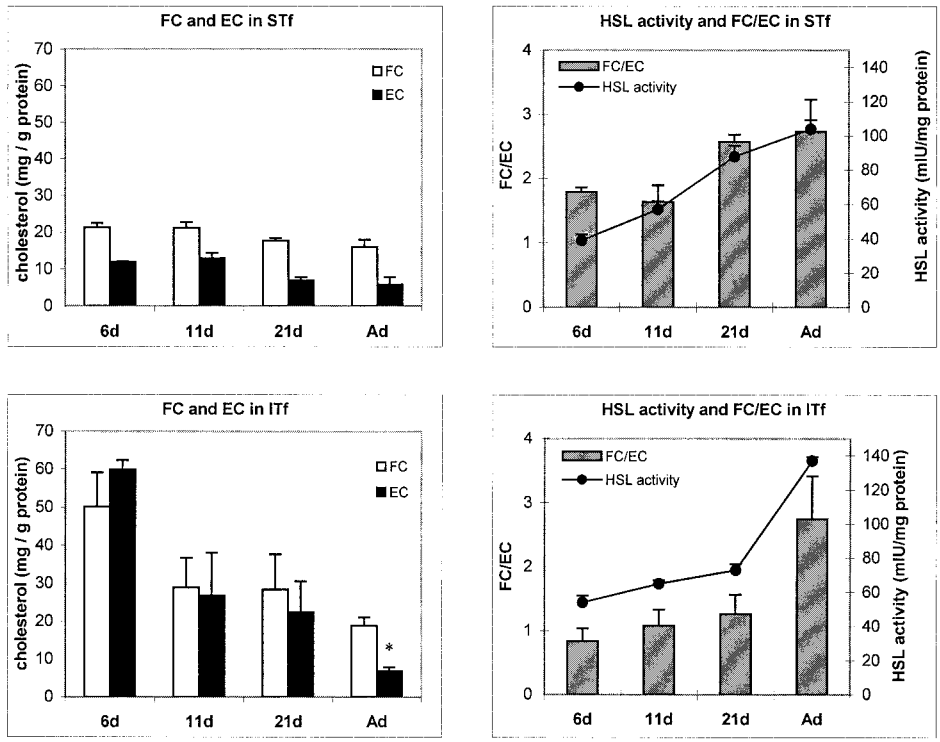

FIG. 6. Testicular FC and EC levels and HSL activity during postnatal testicular development. Total lipids in the STf and ITf obtained from 6-, 11-, and 21-day-old as well as adult testes were extracted. The FC and EC were separated by TLC and quantified by gas-liquid chromatography. The FC and EC are expressed as mg cholesterol/g total protein. Values shown are the mean ± SEM of three independent experiments. The FC and EC concentrations decreased with testicular development in the STf and ITf, but this decrease was significant only for EC in the ITf of adult testes (*$P < 0.05$ vs. 6-day-old sample). The FC:EC ratios were calculated and compared with the HSL activity in the same STf and ITf. The HSL activity paralleled the FC:EC ratios in the STf ($r = 0.80$, $P < 0.01$, n = 10) and in the ITf ($r = 0.71$, $P < 0.05$, n = 10).

Serum Levels of Testosterone

The serum testosterone levels were determined by ELISA and compared with the HSL activity and the relative HSL protein levels. Figure 8 shows that serum testosterone levels decreased significantly with the onset of puberty (11-day-old group) up to 21 days after birth, relatively to the level recorded during the neonatal period (6-day-old group) ($P < 0.05$). Testosterone levels were increased significantly in the adult ($P < 0.001$). The serum testosterone levels correlated with the changes recorded in the HSL activity in the ITf ($r = 0.91$, $P < 0.001$, n = 12) and STf ($r = 0.60$, $P < 0.05$, n = 12) and with the changes in HSL protein levels in ITf ($r = 0.89$, $P < 0.001$, n = 12) and STf ($r = 0.97$, $P < 0.001$, n = 12).

HSL Immunolocalization in Tissue Sections

Controls performed using the second antibody alone or preimmune serum showed no reaction product (Fig. 9a). The HSL immunohistochemical localization was performed with the same antibody used in the Western blot analyses. The HSL was detected in the Sertoli cells in all age groups studied (Fig. 9, b–h), including in neonatal group before the onset of puberty (Fig. 9b). The HSL was localized in elongating spermatids and Sertoli cells, where its distribution was stage-specific in the adult testis (Fig. 9, f–h). The HSL immunoreactivity was most intense in tubules at stage X of the cycle of the seminiferous epithelium following the release of mature spermatids into the lumen, when the HSL immunoreactivity accumulated near the base of the Sertoli cells (Fig. 9g). The HSL was detected in the endothelial cells lining blood vessels within the interstitial tissue of the testis (Fig. 10a). Within the excurrent ducts, HSL immunoreactivity was most intense in cells lining the tubuli recti or straight tubules and the rete testis (Figs. 10, b and c). The HSL labeling was moderate within the epididymis (Fig. 10, d–g).

Localization of HSL in Epididymal Spermatozoa by Immunofluorescence

Controls performed with preimmune serum showed nonspecific labeling in the midpiece of the tail of epididymal spermatozoa (Fig. 11a). The HSL localized principally to the equatorial segment of the head (Fig. 11b) and, occasionally, in the posterior acrosomal segment of spermatozoa.

DISCUSSION

Contribution of cholesterol to the tubules requires the action of several enzymes. Sertoli cells reportedly have the capacity to synthesize cholesterol from acetate in vitro [42]. Although no evidence exists that tubules contribute significantly to androgen production in vivo, if the capacity to synthesize cholesterol also exists in vivo, this would require factors to regulate this capacity with the metabolic demands imposed on Sertoli cells by the cyclic production of germ cells. In the normal testis, more than half the germ cells will die by apoptosis before reaching maturity, and many will be phagocytosed by Sertoli cells, leaving accumulations of cellular debris and stacks of FC-rich, germ cell-born membranes in lysosomes [43]. Despite this contribution of cholesterol to Sertoli cells, because cholesterol is a component of all germ cell membranes, including spermatozoa [44, 45], the cyclical release of spermatozoa offers a constant challenge to the homeostasis of FC in the tubules that demands the action of regulatory mechanisms. The Sertoli cells are involved in the cyclical phagocytosis of EC-rich lipid droplets [43] contained within the spermatids' residual bodies. It has been suggested, yet never shown, that Sertoli cell phagosomes contain esterases and lipases, and that these would process lipids borne by residual bodies and liberate the subunits or ''building blocks'' necessary for new lipid synthesis [46]. The present study addresses, to our knowledge for the first time, the question of the

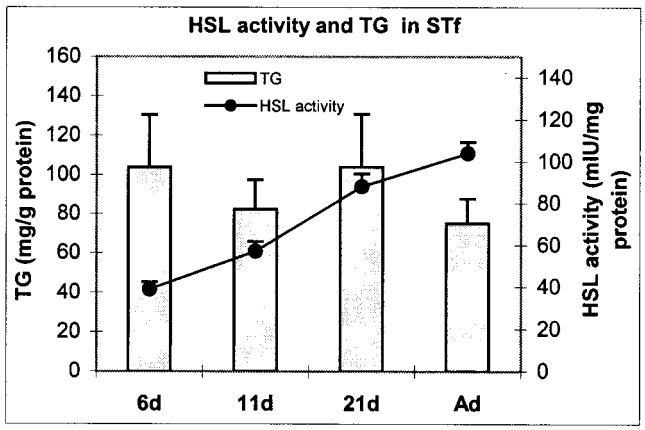

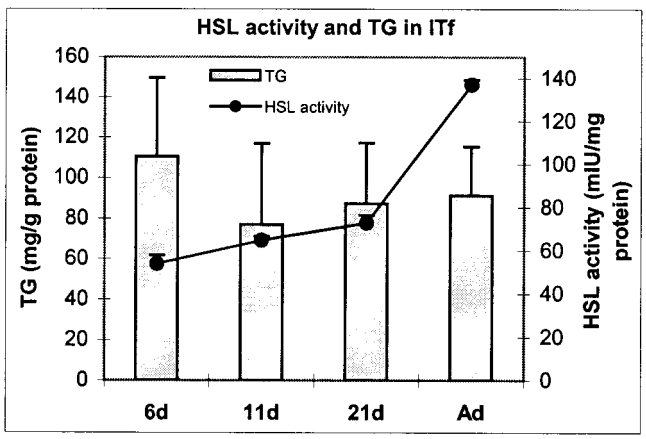

FIG. 7. Triglyceride (TG) levels and HSL activity in the STf and ITf during postnatal testicular development. The TG were assayed in the STf and ITf prepared from 6-, 11-, and 21-day-old as well as adult testes. Values shown are the mean ± SEM of three independent experiments. No significant differences in TG levels were detected throughout testicular development. Comparison of the TG levels and HSL activity in the same testicular fractions from animals of the same age groups showed no correlation between TG levels and HSL activity in both the STf ($r = -0.27$ [not significant]) and ITf ($r = -0.34$ [not significant]).

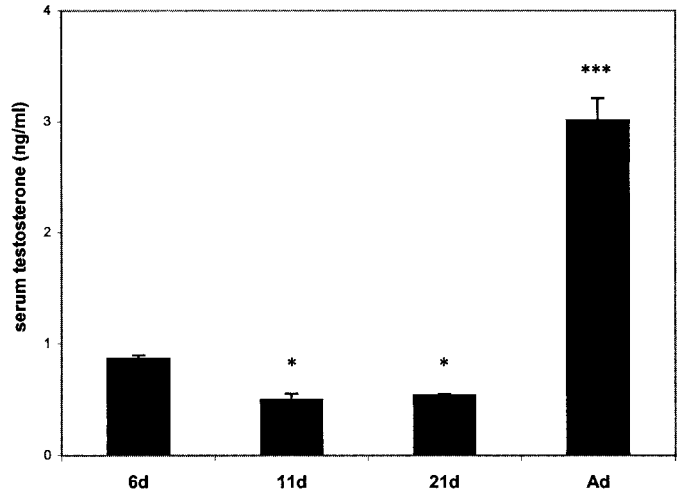

FIG. 8. Serum testosterone concentration during testicular development. Serum testosterone levels were measured by ELISA and expressed as ng/ml. Values shown are the mean ± SEM of five independent experiments. $^{*}P < 0.05$ for 11- and 21-day-old vs. the 6-day-old samples, $^{***}P < 0.001$ adult vs. 6-day-old samples.

putative presence of HSL in Sertoli cell lysosomes. The base of the Sertoli cell is continually exposed to changing plasma cholesterol levels. The suggestion that Sertoli cells possess Apo B and Apo E receptors for the uptake and degradation of low-density and high-density lipoproteins [47] indicates that the supporting cells could actively regulate supplies of cholesterol within the tubules.

The present study substantiates previous reports concerning testicular HSL [10, 13–16]. The detection of guinea pig testicular HSL with larger molecular masses (104, 110, and 120 kDa) than the HSL expressed in other tissues, namely, in the adipose tissue (90 kDa), is in agreement with the results of studies in other species [10, 15, 16, 48]. In addition, because measurements were made here using enriched tissue fractions born of distinct compartments of the testis rather than whole-testis extracts, as used in previous studies, the results extend over other studies and show that HSL activity rather than HSL protein levels was higher in ITf than in STf in the adult. Moreover, the results show that HSL activity and HSL protein levels increased in parallel in both ITf and STf throughout development, except in the STf of the adult, in which the protein levels increased more rapidly than the enzymatic activity. Significantly, HSL mRNA reportedly increases in steroidogenic tissues (i.e., adrenal glands and testis) but remains constant in the adipose tissue during development in the rat [14]. Here, assessments of the FC, EC, and TG levels were made using the same fractions in which HSL protein levels and enzymatic activity were measured. The results show that FC and EC levels decreased in both the interstitial tissue and the tubules during development. The results also show that FC:EC ratios were approximately the same in ITf and STf in the adult (approximately three), but that they were near two in the STf and near one in the ITf during the early phase of development. These results suggest a regulation of cholesterol esterification/de-esterification in the two cellular compartments of the testis during adulthood different from that during development. They also suggest a difference in this regulation of cholesterol esterification/de-esterification in each compartment, at least during the early phase of development. In addition, the results show that a sharp increase in testosterone secretion was accompanied by a decrease in EC in the ITf and by an increase in HSL activity, coincidentally with a decrease in the number of lipid droplets in the Leydig cells (unpublished data) in the adult.

The finding that guinea pig Leydig cells were not positively labeled by antibodies against recombinant rat HSL in the present study could be interpreted in one of two ways. Either no HSL is in the Leydig cells, or the amount of HSL present in the cell is less than the detection limit allowed by the immunohistochemical technique used in this study. Based on the observation of FC and EC levels that are larger in guinea pig ITf than in the STf throughout development (except in the adult, in which these levels are roughly the same), the finding of a significantly higher HSL activity in the ITf than in the STf of all age groups, and our recent unpublished observation of HSL-positive Leydig cells in mink testis, the second alternative is greatly favored. If the suggestion shows itself to be correct, this would support to the notion that HSL may play a role in providing adequate amounts of FC for use by Leydig cells as a precursor of the testosterone necessary for the success of spermatogenesis. In addition, the present finding of a strong, positive correlation of HSL activity with FC:EC ratios in both ITf and STf provides additional support to the

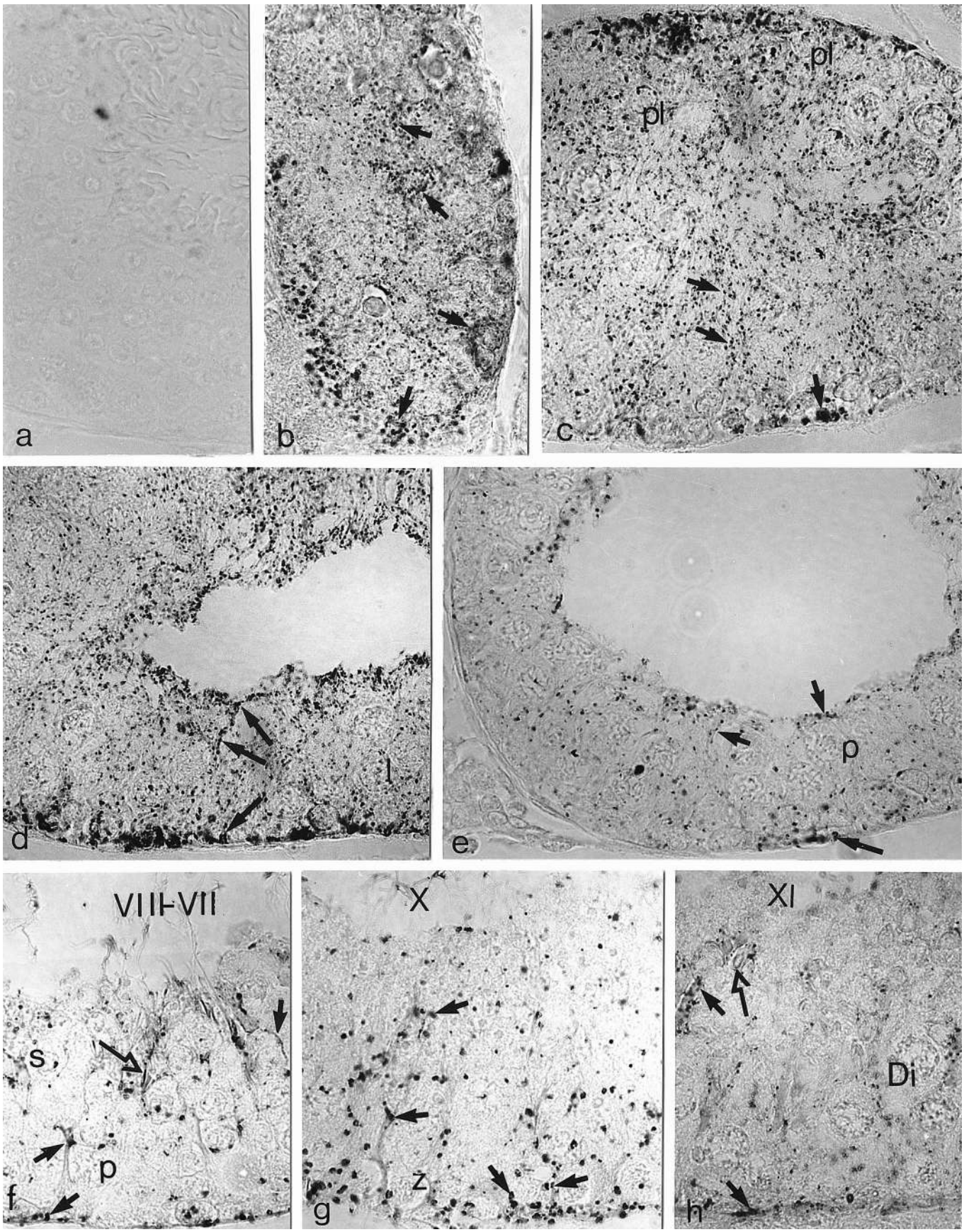

FIG. 9. Immunohistochemical localization of HSL in developing testes. Tissue sections (**a**) incubated with preimmune serum or with the second antibody alone showed no reaction product. The HSL immunolabeling was detected in Sertoli cells from 6 (**b**)-, 11 (**c**)-, 14 (**d**)-, and 21-day-old guinea pigs (**e**). The HSL immunoreactivity was observed within the epithelium throughout development (**b–e**). In the adult testis (**f–h**), HSL was detected in the elongating spermatids (open arrows) and Sertoli cells (closed arrows), in which the enzyme was distributed in minute accumulations throughout the cell and the distribution of the HSL immunoreactivity varied in a stage-specific manner, being most intense in stage X following the release of mature spermatozoa

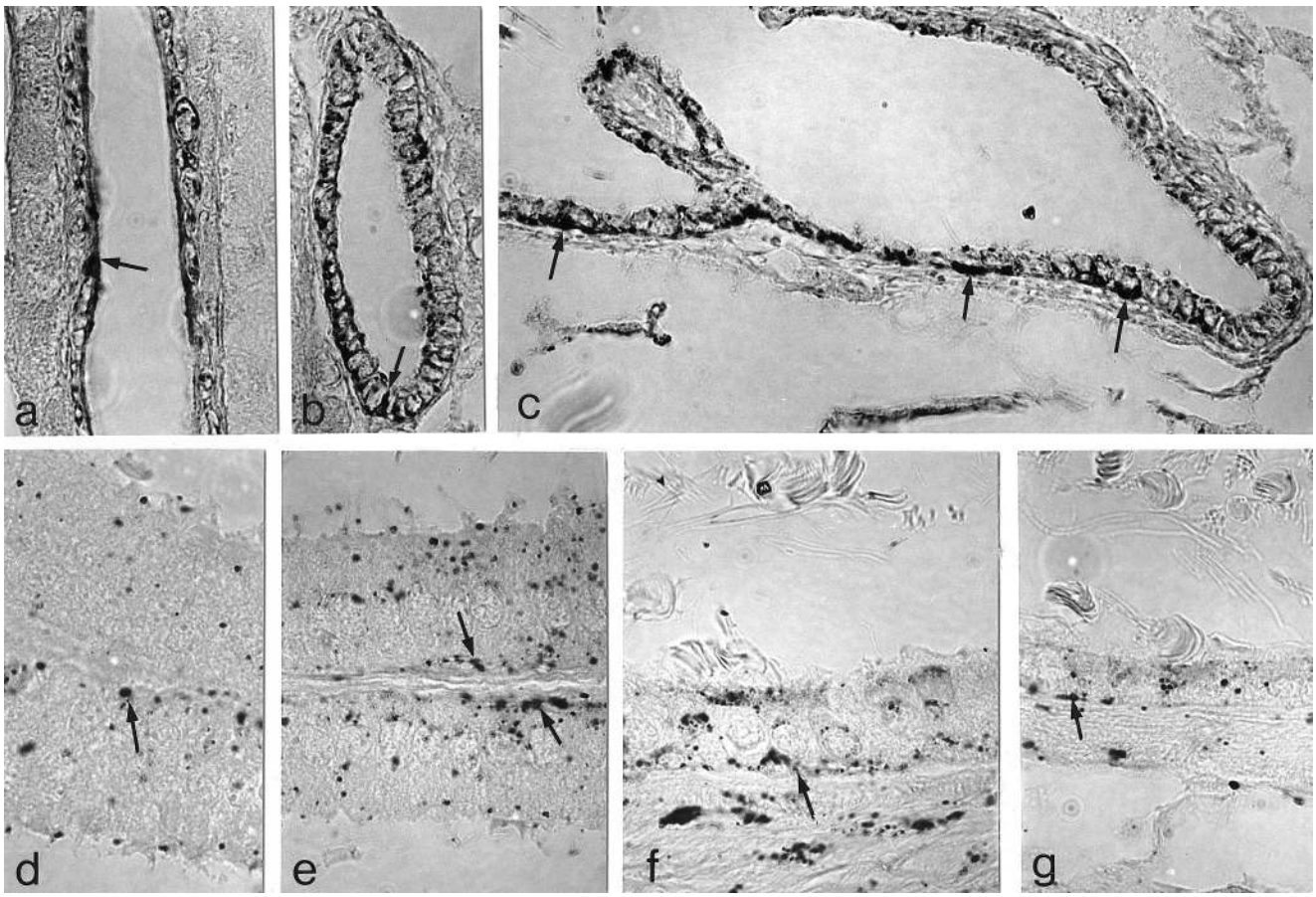

FIG. 10. Immunolocalization of HSL in the interstitial tissue of the adult testis and adult testicular excurrent ducts. The HSL immunoreactivity was intense in the endothelial cells lining the blood vessels (arrow) of the interstitial tissue (**a**). Within the testicular excurrent ducts, the reaction was most intense (arrow) in the cells of the tubuli recti (or straight tubules) (**b**) and of the rete testis (**c**). From the head (**d**) to the tail regions (**g**) of the epididymis, the usual characteristic changes, such as decreased epithelial height and decreased height of stereo cilia, were noticed. The HSL labeling was heaviest in the distal part of the body (**e**) and in the proximal part of the tail (**f**) of the epididymis. ×780.

notion that HSL is the only cholesterol ester hydrolase in this tissue, and that the FC:EC ratios and the enzymatic activity measured in this study using PNPB as substrate reflect the activity of HSL in the STf, ITf, and spermatozoa. The HSL exhibits both cholesterol ester and TG hydrolase activities [49], and the activity of HSL toward cholesterol esters roughly equals that toward triacylglycerol in rat adipose tissue [49]. The finding here that testicular HSL enzymatic activity correlated with tubular and interstitial FC:EC ratios, but not with TG levels, is in agreement with the report that HSL−/− knockout mice possessed no cholesterol esterase activity but did possess residual TG lipase activity in the testis [4].

Here, all measurements were performed during the neonatal period, puberty, and adulthood, thus allowing for correlation of a physiological event typical either to the interstitial tissue or the tubules with a particular phase of testicular development, namely, a peak in serum testosterone levels in the adult and meiosis during puberty. The present study recorded an increase in HSL protein levels and activity in STf that coincided with periods (i.e., the 21-day-old and adult groups) characterized by numerous pachytene

in the lumen of the tubule, when the enzyme accumulated near the base of the Sertoli cells (**g**). A sharp decrease was found in the HSL immunoreactivity coincidental to the appearance of older classes of spermatocytes such as the diplotene spermatocytes during stage XI (**h**). The HSL immunoreactivity was low for the remaining stages of the cycle of the seminiferous epithelium. The stages of the cycle are indicated in roman numerals. Di, Diplotene spermatocytes; l, leptotene spermatocytes; p, pachytene spermatocytes; pl, preleptotene spermatocytes. ×780.

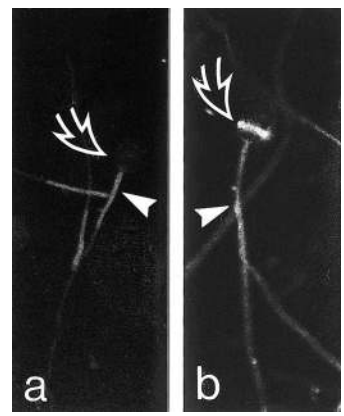

FIG. 11. Immunofluorescence localization of HSL in epididymal spermatozoa. **a**) Epididymal spermatozoa incubated with preimmune serum (control) showed a weak labeling in the midpiece of the tail (arrowhead); however, the remainder of the cell, including the head (open curved arrow), showed no labeling. **b**) The HSL immunolabeling was detected in the equatorial segment of epididymal spermatozoa (open curved arrow). In the midpiece, the nonspecific labeling was similar to the one obtained when the preimmune serum was used (arrowhead). ×780.

spermatocytes in the tubules, reflecting intense meiotic activity. Moreover, the finding of a decrease in HSL labeling coincidental to the appearance of diplotene spermatocytes within the adult seminiferous epithelium hints at a link of HSL with a particular class of germ cells, namely, the spermatocytes. In addition, the present finding of increased HSL immunoreactivity in the tubules during stage X (i.e., two stages of the cycle of the seminiferous epithelium posterior to the release of mature spermatids in the lumen) suggests a role of HSL in the processing of lipids borne by residual bodies. In the present study, HSL accumulated near the base of Sertoli cells in stages following the release of spermatids. This distribution of the enzyme coincides with an increase in lipid droplets that has been documented in the same location and during the same stages of the cycle in other species [46, 50, 51]. However, other morphometric analyses have stressed that although EC-containing lipid droplets increased in tubules coincidental to the release of mature spermatids during spermiation, their numbers were maximal during the stages of the cycle of the seminiferous epithelium that were associated with meiosis [46]. Several pathological conditions leading to an arrest of spermatogenesis at the pachytene spermatocyte stage were reportedly accompanied by an accumulation of lipid droplets in Sertoli cells [52, 53]. In HSL−/− knockout mice, the cholesterol esters are increased [4]. The HSL may play a role in cholesterol mobilization during spermatogenesis. The finding here of the 104- and 120-kDa HSL immunoreactive bands, of measurable HSL activity in spermatozoa, and of the 104-, 110-, and 120-kDa bands in the lysosome subfraction of the adult testes, in which the enzyme is presumably not active (because HSL has an optimum pH of 7), suggests that part of HSL may originate from germ cells and be imported by Sertoli cells.

Using subfractions of STf, the present study provides, to our knowledge for the first time, evidence that testicular HSL is localized in the cytosol, sER, and lysosomes of Sertoli cells. The 110- and 120-kDa immunoreactive bands in the lysosomal subfraction from the STf obtained from adult guinea pig testis may correspond to the 113- and 127-kDa proteins typically reported in mature rat testis [10]. That the 110- and 120-kDa bands were not detected in the ITf of the adult indicates that the enriched tissue fractions used in this study were not contaminated with each other. Moreover, despite the small but unavoidable contamination of the enriched subcellular fractions with other subfractions, the finding of the HSL immunoreactive bands of 104-, 110-, and 120-kDa only in the lysosomal subfraction and the detection of the 104-kDa band in the cytosol subfraction as well as of traces of the 104-kDa in the sER subfraction indicate that the contamination level with other subfractions was lower than the detection limit of the HSL allowed by Western blotting. Other studies have reported that the testis contains two additional large bands [10, 13], but this is the first report showing that the bands are present principally within the tubules. The HSL has been reported to be a cytosolic enzyme [54–56], and our finding of a 104-kDa band in the cytosol is in agreement with the results of these earlier reports. The trace levels of a 104-kDa band detected in association with the sER subfraction may suggest a possible involvement of the enzyme in the lipid metabolism at this location. The present study contributes the first evidence that Sertoli cell lysosomes contain all three HSL immunoreactive bands. The lysosomal HSL likely originates from Sertoli cells, because except for the step 7 spermatids, and unlike Sertoli cells, the germ cells were reported to contain no lysosomes [57]. In this study, the HSL relative protein levels paralleled HSL activity in STf for up to 21 days after birth, whereas in the adult, the increase in enzymatic activity did not correlate with protein expression, suggesting the accumulation of part of the enzyme in lysosomes. This could explain, in part, the relatively low activity of the enzyme in tubules of the adult testis, because HSL is inactive at lysosomal pH.

The finding of HSL in guinea pig Sertoli cells as well as in elongating spermatids is in agreement with those of other immunocytochemical [16] and in situ hybridization studies in the rat [15]. Testicular HSL mRNA has been reported in mouse round spermatids [58]. Transcription could be initiated in round spermatids and translation in elongating spermatids. The present findings of a 104- and 120-kDa HSL immunoreactive bands in spermatozoa and of HSL enzymatic activity in epididymal spermatozoa support the notion that the enzyme plays a role in regulating the proportion of cholesterol relative to other classes of lipids in the plasma membrane of spermatozoa consistent with the acquisition of fertility. Moreover, the present original localization of HSL by immunofluorescence to the equatorial segment of epididymal spermatozoa is consistent with a role in spermatozoa-oocyte interaction. Cholesterol levels were increased in spermatozoa during maturation in the epididymis [59, 60] and decreased during capacitation [61], and this parameter is reportedly associated with the induction of progressive motility and fertility in male gametes [62]. More significantly, a disruption in the proportion of membrane cholesterol in spermatozoa has been identified to be a cause of infertility in the human [63], which gives new impetus to the research concerning the impact of testicular HSL on male fertility.

A temperature-resistant form of cholesterol ester hydrolases has been reported in Sertoli cells and Leydig cells and a temperature-sensitive form of the enzyme only in Sertoli cells in rat testis [39, 40]. This latter form was reported to be active at 32°C, inactive at 37°C, and responsible for an increase in FC:EC ratios in cryptorchid rat testes [39–41, 52]. The guinea pig possesses scrotal testes, yet no differences were recorded in the HSL activity assayed at 34°C, or the physiological temperature of the testis, and in the one assayed at 37°C, or the body temperature, in the present study. Species differences are possible. Birds, for instance, possess intra-abdominal testes, and their testicular HSL likely remains functional at high temperature (i.e., 43–45°C).

In the interstitial tissue of the testis, HSL localized predominantly to the endothelial cells of the blood vessels. One of the surprising results here was that HSL is abundant within testicular endothelial cells but not within Leydig cells or endothelial cells of the epididymis. This suggests that the testicular endothelial cells, which most likely were responsible for the bulk of HSL detected in the interstitial fraction by Western blotting, undergo a maturation process unique to the testis during development. In addition, the present study reports, to our knowledge for the first time, the presence of the enzyme in excurrent ducts of the testis and, in particular, in the cells lining the tubuli recti and the rete testis, where HSL immunoreactivity was intense. The presence of abundant HSL in the tubuli recti is consistent with the localization of HSL in Sertoli cells, because tubuli recti are lined with cells similar to Sertoli cells. The HSL might conceivably be related to the numerous lipid droplets typically found in the excurrent ducts, or the enzyme might play a role in either the testosterone synthesis that has been

documented to take place in this location [64] or the modifications of membrane lipids reported to occur in spermatozoa during their transit through the excurrent ducts [60].

ACKNOWLEDGMENTS

The cholesterol measurements performed in this study could not have been realized without the kind and generous help of Dr. J. Davignon and Dr. S. Lussier-Cacan of the Institute of Clinical Research of Montreal, who not only allowed us the use of their gas-liquid chromatograph but also provided most valuable advice and precious help during the course of this study. Lucie Boulet is thankfully acknowledged for her superb technical assistance. The authors are particularly grateful to Dr. U. Maag from the Department of Mathematics and Statistics of the Université de Montréal for his generous contribution in the treatment of the statistical data. We also thank Dr. J. Paiement from the Department of Pathology and Cell Biology, Université de Montréal, for the use of his facilities and L. Roy for her guidance during the subcellular fractionation. The help of S.R. Yoon in the immunofluorescence studies is also very much appreciated.

REFERENCES

1. Yeaman SJ. Hormone-sensitive lipase—a multipurpose enzyme in lipid metabolism. Biochim Biophys Acta 1990; 1052:128–132.
2. Chang TY, Chang CCY, Cheng D. Acyl-coenzyme A: cholesterol acetyltransferase. Annu Rev Biochem 1997; 66:613–638.
3. Goldstein JL, Brown MS. Regulation of the mevalonate pathway. Nature 1990; 343:425–429.
4. Osuga J, Ishibashi S, Oka T, Yagyu H, Tozawa R, Fujimoto A, Shionoiri F, Yahagi N, Kraemer FB, Tsutsumi O, Yamada N. Targeted disruption of hormone-sensitive lipase results in male sterility and adipocyte hypertrophy, but not in obesity. Proc Natl Acad Sci U S A 2000; 97:787–792.
5. Cook KG, Yeaman SJ, Stralfros P, Belfrage P. Direct evidence that cholesteryl ester hydrolase from adrenal cortex is the same enzyme as hormone-sensitive lipase from adipose tissue. Eur J Biochem 1982; 125:245–249.
6. Cook KG, Colbran RJ, Snee J, Yeaman SJ. Cytosolic cholesterol ester hydrolase from bovine corpus luteum. Its purification, identification, and relationship to hormone-sensitive lipase. Biochim Biophys Acta 1983; 752:46–53.
7. Cordle SR, Colbran RJ, Yeaman SJ. Hormone-sensitive lipase from bovine adipose tissue. Biochim Biophys Acta 1986; 887:51–57.
8. Small CA, Goodacre JA, Yeaman SJ. Hormone-sensitive lipase is responsible for the neutral cholesterol ester hydrolase activity in macrophages. FEBS Lett 1989; 247:205–208.
9. Small CA, Yeaman SJ, West DW, Clegg RA. Cholesterol ester hydrolysis and hormone-sensitive lipase in lactating rat mammary tissue. Biochim Biophys Acta 1991; 1082:251–254.
10. Kraemer FB, Patel S, Saedi MS, Sztalryd C. Detection of hormone-sensitive lipase in various tissues. I. Expression of an HSL/bacterial fusion protein and generation of anti-HSL antibodies. J Lipid Res 1993; 34:663–671.
11. Bartke A, Musto N, Caldwell BV, Behrman HR. Effects of a cholesterol esterase inhibitor and of prostaglandin $F_{2\alpha}$ on testis cholesterol and on plasma testosterone in mice. Prostaglandins 1973; 3:97–104.
12. Bartke A. Concentration of free and esterified cholesterol in the testes of immature and adult mice. J Reprod Fertil 1971; 25:153–156.
13. Holm C, Belfrage P, Fredrikson G. Immunological evidence for the presence of hormone-sensitive lipase in rat tissues other than adipose tissue. Biochem Biophys Res Commun 1987; 148:99–105.
14. Kraemer FB, Tavangar K, Hoffman AR. Developmental regulation of hormone-sensitive lipase mRNA in the rat: changes in steroidogenic tissues. J Lipid Res 1991; 32:1303–1310.
15. Stenson Holst L, Hoffman AR, Mulder H, Sundler F, Holm C, Bergh A, Fredrikson G. Localization of hormone-sensitive lipase to rat Sertoli cells and its expression in developing and degenerating testes. FEBS Lett 1994; 355:125–130.
16. Stenson Holst L, Langin D, Mulder H, Laurell H, Grober J, Bergh A, Mohrenweiser HW, Edgren G, Holm C. Molecular cloning, genomic organization, and expression of a testicular isoform of hormone-sensitive lipase. Genomics 1996; 35:441–447.
17. Osterlund T, Danielsson B, Degerman E, Contreras JA, Edgren G, Davis RC, Schotz MC, Holm C. Domain-structure analysis of recombinant rat hormone-sensitive lipase. Biochem J 1996; 319:411–420.
18. De Duve C, Pressman BC, Gianetto R, Wattiaux R, Appelmans F. Tissue fractionation studies. 6. Intracellular distribution pattern of enzymes in rat liver tissue. Biochem J 1955; 60:604–617.
19. Wattiaux R, Wattiaux-De-Coninck S, Ronveaux-Dupal M, Dubois F. Isolation of rat liver lysosomes by isopycnic centrifugation in a metrizamide gradient. J Cell Biol 1978; 78:349–368.
20. Igdoura SA, Morales CR. Role of sulfated glycoprotein-1 (SGP-1) in the disposal of residual bodies by Sertoli cells of the rat. Mol Reprod Dev 1995; 40:91–102.
21. Bergeron JJM, Rachubinski RA, Sikstrom RA, Posner BI, Paiement J. Galactose transfer to endogenous acceptors within Golgi fractions of rat liver. J Cell Biol 1982; 92:139–146.
22. Paiement J, Bergeron JJM. Localization of GTP-stimulated core glycosylation to fused microsomes. J Cell Biol 1983; 96:1791–1796.
23. Roy AB. The sulphatase of ox liver. I. The complex nature of the enzyme. Biochem J 1953; 53:12–15.
24. Graham JM. The identification of subcellular fractions from mammalian cells. In: Graham JM, Higgins JA (eds.), Methods in Molecular Biology, vol. 19: Biomembrane Protocols: I. Isolation and Analysis. Totowa, NJ: Humana Press; 1993: 1–18.
25. Ames RN, Dubin DT. The role of polyamines in the neutralization of bacteriophages deoxyribonucleic acid. J Biol Chem 1960; 235:769–775.
26. Davis GA, Bloom FE. Subcellular particles separated through a histochemical reaction. Anal Biochem 1973; 51:429–435.
27. Herrada G, Wolgemuth DJ. The mouse transcription factor Stat4 is expressed in haploid male germ cells and is present in the perinuclear theca of spermatozoa. J Cell Sci 1997; 110:1543–1553.
28. Bradford MM. A rapid and sensitive method for the quantitation of microgram quantities of protein utilizing the principle of protein-dye binding. Anal Biochem 1976; 72:248–254.
29. Pelletier R-M, Trifaró J-M, Carbajal ME, Okawara Y, Vitale ML. Calcium-dependent actin filament-severing protein scinderin levels and localization in bovine testis, epididymis, and spermatozoa. Biol Reprod 1999; 60:1128–1136.
30. Towbin H, Staechelin T, Dordon J. Electrophoretic transfer of proteins from polyacrylamide gels to nitrocellulose sheets: procedure and some applications. Proc Natl Acad Sci U S A 1979; 76:4350–4354.
31. Christensen AK. The fine structure of testicular interstitial cells in guinea pigs. J Cell Biol 1965; 26:911–935.
32. Pelletier R-M. The distribution of connexin 43 is associated with the germ cell differentiation and with the modulation of the Sertoli cell junctional barrier in continual (guinea pig) and seasonal breeders' (mink) testes. J Androl 1995; 16:400–409.
33. Pelletier R-M, Okawara Y, Vitale ML, Anderson JM. Differential distribution of the tight-junction-associated protein ZO-1 isoforms $\alpha+$ and $\alpha-$ in guinea pig Sertoli cells: a possible association with f-actin and g-actin. Biol Reprod 1997; 57:367–376.
34. Clermont Y. Cycle of the seminiferous epithelium of the guinea pig: a method for identification of the stages. Fertil Steril 1960; 11:563–573.
35. Holm C, Osterlund T. Hormone-sensitive lipase and neutral cholesteryl ester lipase. In: Doolittle MH, Reue K (eds.), Methods in Molecular Biology, vol. 109: Lipase and Phospholipase Protocols. Totowa, NJ: Humana Press; 1999: 109–121.
36. Oram JF. Receptor-mediated transport of cholesterol between cultured cells and high-density lipoproteins. In: Albers JJ, Segrest JP (eds.), Methods in Enzymology, vol. 129. London: Academic Press; 1986: 645–659.
37. Brown MS, Faust JR, Goldstein JL. Role of the low density lipoprotein receptor in regulating the content of free and esterified cholesterol in human fibroblasts. J Clin Invest 1975; 55:783–793.
38. Noller DW, Flickinger CJ, Howard SS. Duration of the cycle of the seminiferous epithelium in the guinea pig determined by tritiated thymidine autoradiography. Biol Reprod 1977; 17:532–534.
39. Durham LA, McLean Grogan W. Temperature sensitivity of cholesteryl ester hydrolases in the rat testis. Lipids 1982; 17:970–975.
40. Durham LA, McLean Grogan W. Characterization of multiple forms of cholesteryl ester hydrolase in the rat testis. J Biol Chem 1984; 259: 7433–7438.
41. Wee S, McLean Grogan W. Testicular temperature-labile cholesteryl ester hydrolase. J Biol Chem 1993; 268:8158–8163.
42. Wiebe JP, Tilbe KS. De novo synthesis of steroids (from acetate) by isolated rat Sertoli cells. Biochem Biophys Res Commun 1979; 89: 1107–1113.
43. Pelletier R-M, Vitale ML. Filipin vs enzymatic localization of choles-

terol in guinea pig, mink, and mallard duck testicular cells. J Histochem Cytochem 1994; 42:1539–1554.
44. Pelletier R-M, Friend DS. Development of membrane differentiations in the guinea pig spermatid during spermiogenesis. Am J Anat 1983; 167:119–141.
45. Pelletier R-M, Shivers RR. Filipin-sterol complexes in breeding and non-breeding (*Mustela vison*) Sertoli cell junctional membranes. J Cell Biol 1986; 103:365–365.
46. Kerr JB, Mayberry RA, Irby DC. Morphometric studies on lipid inclusions in Sertoli cells during the spermatogenic cycle in the rat. Cell Tissue Res 1984; 236:699–709.
47. Maboundou J-C, Fofana M, Fresnel J, Bocquet J, LeGoff D. Effect of lipoproteins on cholesterol synthesis in rat Sertoli cells. Biochem Cell Biol 1995; 73:67–72.
48. Large V, Arner PR, Reynisdottir S, Grober J, Van Harmelen V, Holm C, Langin D. Hormone-sensitive lipase expression and activity in relation to lipolysis in human fat cells. J Lipid Res 1998; 39:1688–1695.
49. Fredrikson G, Stralfros P, Nilsson O, Belfrage P. Hormone-sensitive lipase of rat adipose tissue. J Biol Chem 1981; 256:6311–6320.
50. Niemi M, Kormano M. Cyclical changes in and significance of lipids and acid phosphatase activity in the seminiferous tubules of the rat testis. Anat Rec 1965; 151:159–170.
51. Kerr JB, de Kretser DM. Cyclic variations in Sertoli cell lipid content throughout the spermatogenic cycle in the rat. J Reprod Fertil 1975; 43:1–8.
52. Johnson AD. Testicular lipids. In: Johnson AD, Gomes WR, Vandemark NL (eds.), The Testis, vol. 2. New York: Academic Press; 1970: 194–258.
53. Chung KW, Hamilton JB. Testicular lipids in mice with testicular feminization. Cell Tissue Res 1975; 160:69–80.
54. Egan JJ, Greenberg AS, Chang M-K, Wek SA, Moos MC, Londos C. Mechanism of hormone-stimulated lipolysis in adipocytes: translocation of hormone-sensitive lipase to the lipid storage droplet. Proc Natl Acad Sci U S A 1992; 89:8537–8541.
55. Carey GB. Mechanisms regulating adipocyte lipolysis. Adv Exp Med Biol 1998; 441:157–170.
56. Clifford GM, Londos C, Kraemer FB, Vernon RG, Yeaman SJ. Translocation of hormone-sensitive lipase and perilipin upon lipolytic stimulation of rat adipocytes. J Biol Chem 2000; 275:5011–5015.
57. Hermo L, Oko R, Morales CR. Secretion and endocytosis in the male reproductive tract: a role in sperm maturation. Int Dev Cytol 1994; 154:106–189.
58. Blaise R, Grober J, Rouet P, Tavernier G, Daegelen D, Langin D. Testis expression of hormone-sensitive lipase is conferred by a specific promoter that contains four regions binding testicular nuclear proteins. J Biol Chem 1999; 274:9327–9334.
59. Parks JE, Hammerstedt RH. Developmental changes occurring in the lipids of ram epididymal spermatozoa plasma membrane. Biol Reprod 1985; 32:653–668.
60. Rana APS, Majumder GC, Misra S, Ghosh A. Lipid changes of goat sperm plasma membrane during epididymal maturation. Biochim Biophys Acta 1991; 1061:185–196.
61. Go KJ, Wolf D. The role of sterols in sperm capacitation. Adv Lipid Res 1983; 20:317–330.
62. Haidl G, Opper C. Changes in lipids and membrane anisotropy in human spermatozoa during epididymal maturation. Hum Reprod 1997; 12:2720–2723.
63. Sugkraroek P, Kates M, Leader A, Tanphaichitr N. Level of cholesterol and phospholipids in freshly ejaculated sperm and Percoll-gradient-pelleted sperm from fertile and unexplained infertile men. Fertil Steril 1991; 55:820–827.
64. Robaire B, Hermo L. Efferent ducts, epididymis, and vas deferens: structure, functions, and their regulation. In: Knobil E, Neill JD (eds.), The Physiology of Reproduction, vol. 1. New York: Raven Press; 1988: 999–1080.